**MSc in Photonics**

PHOTONICS**BCN**

Universitat Politècnica de Catalunya (UPC)
Universitat Autònoma de Barcelona (UAB)
Universitat de Barcelona (UB)
Institut de Ciències Fotòniques (ICFO)

http://www.photonicsbcn.eu

*Master in Photonics*

# MASTER THESIS WORK

# COMPACT TUNABLE AND RECONFIGURABLE MICROWAVE PHOTONIC FILTER FOR SATELLITE PAYLOADS

**Oraman Yoosefi**

**Supervised by Dr. Maria Santos, (UPC)**

Presented on date 08th July 2015

Registered at

Escola Tècnica Superior d'Enginyeria de Telecomunicació de Barcelona

## 1. INTRODUCTION

Microwave photonics is basically concerned with photonic subsystems designed with the aim of carrying equivalent tasks to those of an ordinary microwave circuit or system, bringing supplementary advantages inherent to photonics such as low loss, high bandwidth, and immunity to electromagnetic interference (EMI), tunability, and reconfigurability. The term microwave will be freely used throughout this paper to designate RF, microwave, or millimeter-wave signals. Among the expected benefits of microwave signal processing in the optical domain are wide bandwidth operation, reduced weight and volume, immunity to electromagnetic interference and added functionalities such as simple and dynamic tunability and reconfigurability [1-2]. In the recent years an extraordinary advance of photonic technologies mainly spurred by the demand of the telecommunication industry has been witnessed. Worldwide massive fiber-optic network deployments have become an inexhaustible source of a continuous strive for improving performances, reducing cost and complexity and enhancing reliability of photonic components for optical network applications. Examples include tunable lasers, optical filters, amplifiers, modulators and wideband photodiodes (PD). Building on the potential offered by this new generation of photonic components and techniques, a new generation of photonic based solutions to microwave applications with enhanced features is coming to light.

Microwave photonic systems for satellite applications are lately receiving much attention as a new generation of THz capacity telecom satellites is targeted. The Final report of ESA_ARTES-1 activity "Next Generation Telecom Payloads based on Photonic Technologies" contains a comprehensive review of the applicability of microwave photonic approaches to satellite on-board signal processing functions. Among the microwave signal processing functions required on-board satellites, spectral band selection and filtering is particularly challenging, especially for telecom applications where quite often a very narrow electrical pass band is required and tunability and re-configurability are highly appreciated. A number of approaches for the design of filters at microwave frequencies based on photonic technologies, i.e., microwave photonic filters (MPF), has emerged showing tremendous potential in a variety of applications. In MPF the input RF signal is modulated over an optical carrier, processed in the optical domain, and then photodetected to provide the filtered RF output. Very comprehensive reviews of the topic of microwave photonic filtering can be found in [3-4].

We present a novel approach for the photonic filtering of microwave signals based on a direct-synthesis technique with optical phase modulation of the microwave signal and employing two tunable laser sources and a fixed optical passband filter. Both center frequency and bandwidth of the MPF may be controlled independently by proper selection of the respective laser wavelength detunings with respect to the filter cutoff's and therefore wide bandwidth fixed optical filters may be employed irrespective of the required MPF center frequency and bandwidth. Owing to its direct-synthesis nature, the proposed MPF enjoys the advantages of single passband response and reduced noise levels, in a simple and compact setup. Experimental measures are provided to support the feasibility of the method along with simulated results based on Virtual Photonics Inc. (VPI) that show its potential.

The paper is structured as follows. We start with an overview of the state of the art in Photonic Filtering techniques followed by a description of the basic MPF setup and its principle of operation. Next, in section III, the simulation procedures along with the results obtained, are shown and analyzed. In section IV we present the experimental setup and the measurements made and finally section V summarizes the main conclusions derived from the work.

## 2. STATE OF THE ART IN PHOTONIC MICROWAVE FILTERING

A first subclass of MPF is based on discrete-time signal processing [5] which may in turn be broadly subdivided into the Finite Impulse Response (FIR) and the Infinite Impulse Response (IIR) types of MPF. FIR filters combine at their output a finite set of delayed and weighted replicas or taps of the input optical signal, while IIR filters are based on recirculating cavities to provide an infinite number of weighted and delayed replicas of the input optical signal. In order to ensure robustness against environmental changes, the overall

majority of the proposed schemes work under the incoherent regime, i.e., the optical delays are much greater than the coherence time of the optical source. A fundamental drawback of incoherent approaches is related to Phase Induced Intensity noise (PIIN) due to the incoherent sum of signals. This is generally the dominant source of noise and it scales with the square of the signal power, just as the signal does, and therefore there are no simple ways of mitigating its effect [4]. It is also important to note that the spectral response of discrete-time MPFs is inherently periodic, where the Free Spectral Range (FSR) is inversely proportional to the tap delay, and usually features a baseband response.

Direct synthesis MPF, on the other hand, which rely on smart combinations of RF modulation of the optical carrier on the one hand, and optical filtering on the other, are capable of providing a single passband, are free from PIIN and feature very simple setups. As being free from the bias-drift problem, strategies based on phase rather than amplitude modulation are preferred. A typical example of Direct-synthesis MPF with phase modulation is found in [6], where use is made of two narrow passband Fiber Bragg Gratings (FBG), whose passbands are tuned such that while one of them selects the optical carrier, their relative spectral distance gives the center frequency of the MPF. A 10 GHz MPF with ~1 GHz bandwidth was reported [6]. Also a tunable center frequency MPF from 18 to 40 GHz and adjustable bandwidth from 5 to 15 GHz has been demonstrated with this arrangement by using temperature tuned silicon on insulator microrings as passband optical filters [7]. A similar approach employs a notch optical filter to cancel one of the sidebands of the optical phase modulation out [8-9]. A narrow-band center-frequency tunable MPF from 1 to 6.5 GHz with bandwidth on the 100 MHz range has been measured using a phase shifted FBG as the notch filter [9], but the MPF bandwidth is fixed and determined by the optical filter bandwidth. In [10] the RF phase modulated optical signal goes through an optical filter so that the frequency detuning of the optical carrier with respect to the optical filter center frequency determines the bandwidth of the MPF, while the MPF center frequency is equal to the semi-bandwidth of the optical filter. Using temperature controlled FBGs and tunable lasers, center frequency tunable MPFs from 8 to 15 GHz with reconfigurable bandwidths on the GHz range have been reported [10].

Regarding the requirements of MPFs of interest, the following advantages can be derived from the use of a coherent direct-synthesis MPF approach: single-passband response; compact, simple, robust and stable setups; use of phase modulation and no requirement of a (bulky) dispersive device. Among the drawbacks we find: inability to implement general RF responses; no systematic approaches available for arbitrary RF response synthesis; no simple and flexible reconfiguration; and finally, the filters Q factor mainly depends on the optical filter BW, which cannot be made too narrow.

## 3. PRINCIPLE OF OPERATION

The basic scheme of the proposed direct-synthesis MPF is depicted in Fig. 1. It comprises two tunable laser sources with wavelengths lying within the passband of an optical filter and which may be adjusted to specific detunings with respect to the optical filter cutoff's. The laser outputs are coupled and fed to a single phase modulator (PM) which imprints the microwave input signal on both carrier wavelengths. After the modulator, the two phase modulated signals are optically filtered and then photodetected to provide the microwave output signal. Since this photodetector is only sensitive to optical envelope fluctuations, no microwave power is obtained whenever the whole double-sideband spectrum of the two optical phase modulated signals is comprised within the optical filter pass band.

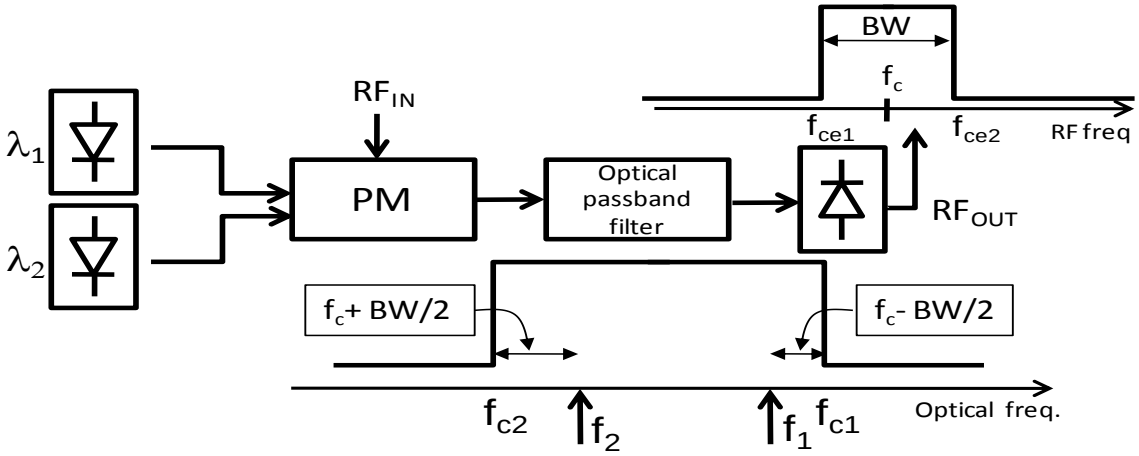


**Fig 2. Schematic representation of the proposed MPF setup**

The microwave photonic passband filtering effect of the described setup is understood as follows. Each of the optical carriers ($f_2$,$f_1$ , with $f_2 < f_1$) is placed respectively close to each of the cutoff wavelengths of the wideband optical filter ($f_{c2}$ ,$f_{c1}$ , with $f_{c2}<f_{c1}$) so that their respective detunings respect to the closest cutoff are different ($df_1 = f_{c1}-f_1 \neq df_2 = f_2- f_{c2}$ ), and their spectral difference $f_1$-$f_2$ is so large that photomixing products among different laser output components fall outside the electrical band of interest. See the sketch in Fig. 2 for reference. The MPF passband frequency cutoffs will be given by $f_{ec1} = \min(df_1,df_2)$, $f_{ec2} = \max(df_1,df_2)$, as explained next and sketched in Fig. 2. For frequencies $f<f_{ec1}$ the whole spectrum of both phase modulated double-sideband optical signals is within the optical passband, and therefore there is no detected microwave signal at the photodiode output. Instead, for $f_{ec1}<f<f_{ec2}$, one of the sidebands of one of the two optical signals is filtered out yielding envelope fluctuations which provide a microwave power after photo detection. For $f>f_{ec2}$, both optical signals lose one of their sidebands, and have a different sign for their remaining sideband. The sidebands photo mixing with the respective optical carriers yields opposing amplitude fluctuations, and therefore if the laser amplitudes are kept equal and the optical filter has a flat passband, very low microwave power levels are obtained for $f>f_{ec2}$, as shown in Fig 2.

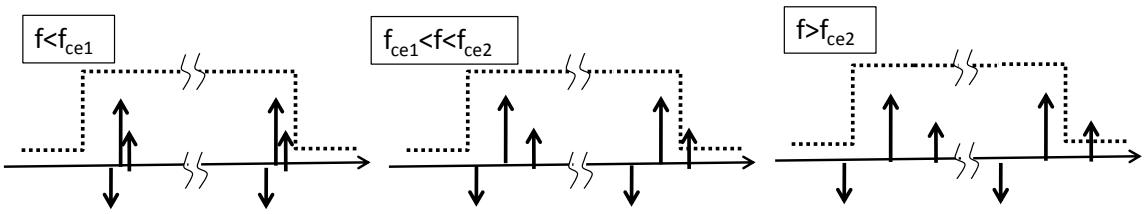


**Fig 1. Sketch of optical spectrum of PM output relative to optical filter spectrum transfer function for different electrical frequency margins**

## 4. SIMULATION RESULTS

Fig. 3 shows the block diagram of the simulated system in VPI. The output power level and linewidth in both lasers are respectively 1mW and 10MHz. In the simulations the effect of uncorrelated phase noise has been accounted for by setting different random number seeds for the phase noise generation. The use of a very low modulation amplitude value in the RF pure sine electrical wave generator ensures a narrow phase modulation spectrum which is expected to provide

better results with the proposed method. In our simulations we have set a safety value of 0.1V, with V the required voltage in the PM for a 180º optical phase shift, but we have checked out that slightly higher values are also appropriate.

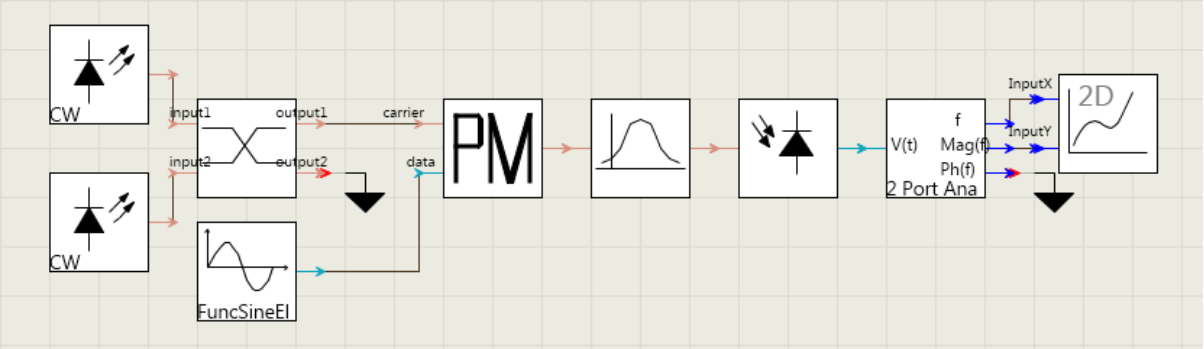


**Fig 3. VPI Simulation setup**

The optical filter is a key element in the MPF setup. As explained, very wide bandwidths and moderately sharp cutoffs are advised. From the many options available in VPI for the optical filter we have selected an idealized trapezoidal transfer function with the minimum phase option active [11], so that the resulting filter is causal and hence physically realizable. Passband and stopband are respectively 500 GHz and 506 GHz, and stopband attenuation is 30 dB. As shown in Fig. 3, a 2 port Analyzer has been connected to the photodiode output with the purpose of recording the photo detected amplitude values at the electrical frequency injected in the system by the electrical sine wave generator. In order to obtain the electrical spectral insertion loss transfer function of such an arrangement, automatic sweeps of the electrical frequency from 200 MHz to 40 GHz in 200 MHz steps have been run. The outcome of a series of simulations considering different values of the two input wavelengths is displayed in Fig. 3.

Fig. 4 (a) shows the results of a variety of input wavelength combinations, all providing 1 GHz bandwidth, and center frequency passband values ranging from 2.5GHz to 35.5GHz. The insertion loss spectral transfer curves have been normalized to 0 dB but in all cases passband insertion loss were around 10 dB for the 1mW power level lasers. The passband insertion loss in any case, scales with the lasers output power level so that even net gain can be obtained in the MPF passband for laser output power level greater than 10 mW. Remarkable passband flat-top responses are observed which are maintained fairly unaltered throughout the broad tunability range. Fairly symmetrical bandpass-bandstop transitions are seen for moderate values of the passband center frequency (8.5 GHz, 12.5 GHz), but while in the lower frequency stopband the attenuation increases monotonically as the frequency is reduced, in the higher frequency stopband an insertion loss floor is reached at around 12 dB stopband attenuation for a 12.5 GHz center frequency passband. This insertion loss floor is seen to drop as the center frequency passband is increased, to reach a maximum stopband attenuation of 15dB at 35 GHz, and it rises up to a stopband attenuation of only 5 dB for 2 GHz center frequency passband. The contrast found between the shapes of the bandstop-passband transitions at the lower and the upper MPF cutoffs is a reflection of the different nature of the filtering mechanisms that take place at each MPF frequency cutoff. While in the lower frequency cutoff the transition from stopband to passband is due to the phase to amplitude conversion that comes from cancellation of one of the sidebands of one of the two phase modulated signals; the upper frequency cutoff occurs because of the destructive interference between the amplitudes detected when both phase modulated signals lose one of their sidebands to the optical filtering. A possible explanation to this is the dispersion

introduced by the filter at the different carrier bands preventing perfect cancellation of the detected signal at each wavelength. Fig. 4 b) shows the capability for selecting a specific bandpass bandwidth of the proposed structure. A similar behaviour is observed with respect to the higher stopband insertion loss floor, i. e. it is seen to rise as the bandpass bandwidth is increased.

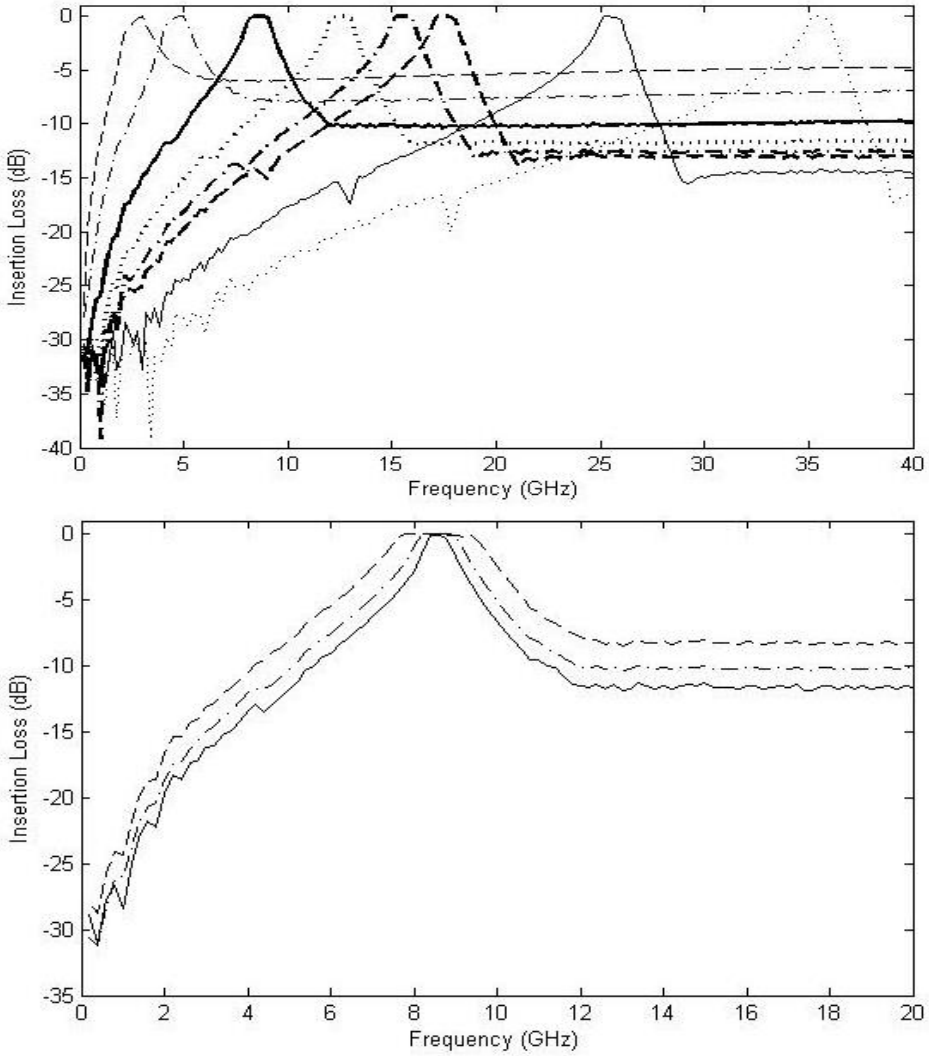


**Fig 4. MPF spectral transfer functions for different laser wavelength detunings ($\Delta f_1$, $\Delta f_2$ ) from the optical filter center frequency passband. a) dashed thin line: $\Delta f_1$=248 GHz, $\Delta f_2$= -247 GHz; dash-dot thin line: $\Delta f_1$=246 GHz, $\Delta f_2$= -245 GHz; solid thick line: $\Delta f_1$=242 GHz, $\Delta f_2$= -241 GHz; dotted thick line: $\Delta f_1$=238 GHz, $\Delta f_2$= -247 GHz; dash-dot thick line $\Delta f_1$=235 GHz, $\Delta f_2$= -234 GHz; dashed thick line: $\Delta f_1$=233 GHz, $\Delta f_2$= -232 GHz; solid thin line: $\Delta f_1$=225 GHz, $\Delta f_2$= -226 GHz; dotted thin line: $\Delta f_1$=215 GHz, $\Delta f_2$= -214 GHz. b) solid line: $\Delta f_1$=241.75 GHz, $\Delta f_2$= -241.25 GHz; dash-dot line: $\Delta f_1$=242 GHz, $\Delta f_2$= -241 GHz; dashed line: $\Delta f_1$=242.5 GHz, $\Delta f_2$= -240.5 GHz**

## 5. EXPERIMENTAL RESULTS

In order to show the practical feasibility of the proposed MPF scheme a experimental setup was assembled, as shown in Fig. 5. It consists of two diode laser sources: a Nortel Networks LC155W-20A Distributed Feedback (DFB) laser module in 14-pin butterfly package with ILX LDC-3724B current and temperature controller, and a New-Focus 6427C external cavity laser (ECL). The broad tunability range of the ECL has been advantageously used in our experiments but in practice telecom-

grade temperature-tuned DFBs may be employed which can be found in the market at very competitive prices. As the phase modulating device, an integrated travelling-wave electro-optical lithium Niobate ($LiNbO_3$) phase modulator (PM) from Covega-Thorlabs, with 35 GHz RF bandwidth and $V_\pi$=5.5V has been used. As a consequence of the intrinsic anisotropy of the $LiNbO_3$ crystal, the modulation efficiency in the PM is dependent upon the direction of polarization of the input optical

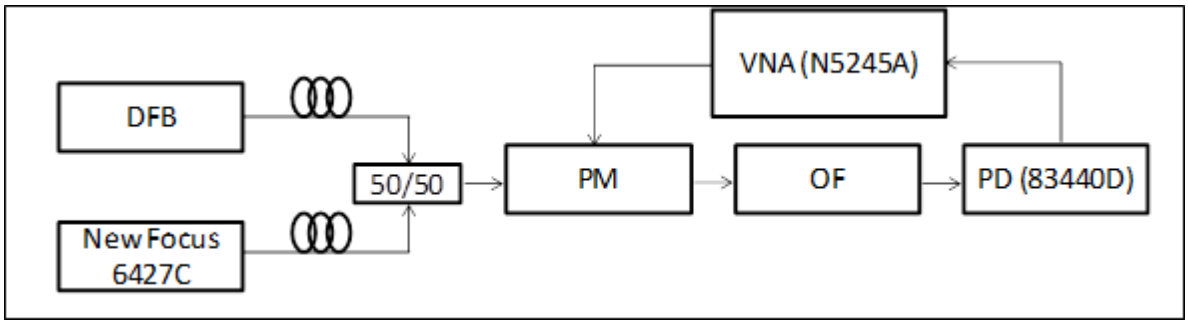


**Fig 5. Experimental setup**

wave and it is maximum when both the optical and the electrical co-propagating waves follow the direction of the optical axis in the uniaxial $LiNbO_3$ crystal [12]. The phase modulator used in the experiment incorporates a polarization maintaining input optical fiber whose axis is oriented in the direction of maximum modulation efficiency, i. e. lower $V_\pi$. One polarization controller (PC) at the output of each laser serves the purpose of ensuring that the optical signals that arrive at the PM are aligned with the input fiber axis. A passive 50/50 optical coupler joins together the signals coming from each laser and transfers them to the input of the PM. After getting the phase modulation inside the PM the two signals pass through the optical filter (OF), which is a 200 GHz bandwidth WDM channel selector with nominal center wavelength at 1547.72 nm corresponding to WDM ITU channel 37. The output of the optical filter goes directly to an Agilent 83440D optical photodetector (PD) Nortel with 10 GHz bandwidth. An Agilent Vectorial Network Analyzer (VNA) N5245A provides the RF MPF input by connecting to the PM electrical contact and retrieves the MPF output from the PD to yield swept frequency S21 insertion loss measurements, from 10 GHz to 50 GHz.

### 5.1 Swept wavelength tests

As a first test for seeing the electrical frequency filtering properties of the system, we employed one laser modulated with a constant electrical frequency of 10 GHz, and swept the optical wavelength of the laser to obtain a plot as shown in Fig 6. This is agreement with the nominal passband of the filter from 1547.10 nm to 1548.43 nm, and allows to more accurately identify the cut-off regions in our setup. Next we fixed the laser wavelength and made electrical frequency swept measurements of insertion loss. As steaming from the analysis in section 3, the one laser measurement should provide

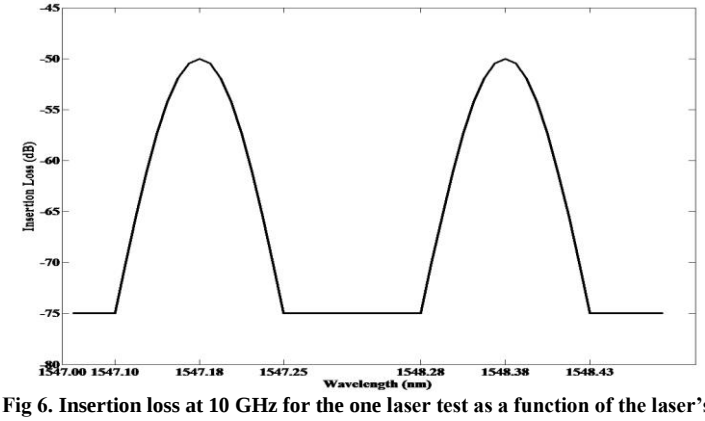


**Fig 6. Insertion loss at 10 GHz for the one laser test as a function of the laser's wavelength 1547.10nm-1548.43nm.**

a high pass characteristic, when the wavelength is close to one of the optical filter cutoffs. Relative to the two cutoff regions shown in Fig 6, Figures 7 and 8 have been obtained in the lowest and highest cutoffs respectively. Also apparent in the figures is the BW limitation of our PD, with a 10 GHz nominal BW.

The best peak insertion loss value in the first cutoff (-47.7 dB) is achieved with λ=1547.18nm (Fig.7) (with a laser power of 6.9 dBm),

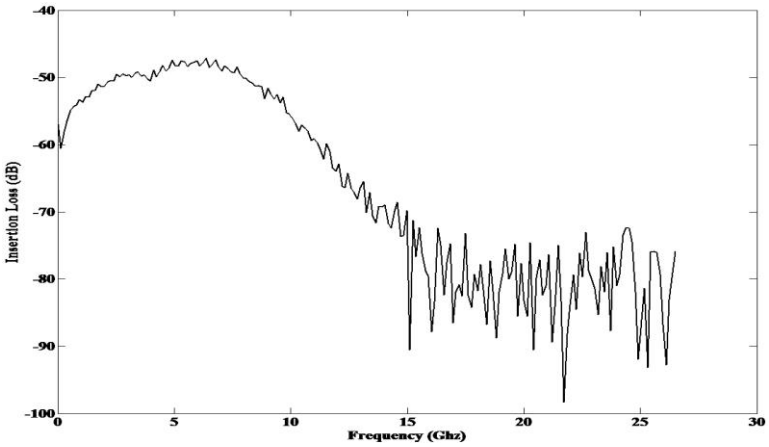


**Fig 7. S21(dB) module NA with wavelength λ=1547.18nm**

The second cut off of the filter is determined by tuning from $\lambda_3$= 1548.28nm, as shown in Fig 8 (from NA) up to $\lambda_4$= 1548.43nm, with -39dB loss. With further tuning, we see that no signal is detected for any electrical frequency meaning the whole spectrum is comprised into the optical filter passband. This test demonstrates the filter is efficient and the two cut offs: first cut off from $\lambda_1$=1547.10nm to $\lambda_2$=1547.25nm and second cut off from $\lambda_3$=1548.28nm to $\lambda_4$= 1548.43nm (laser power =6.9 dBm).

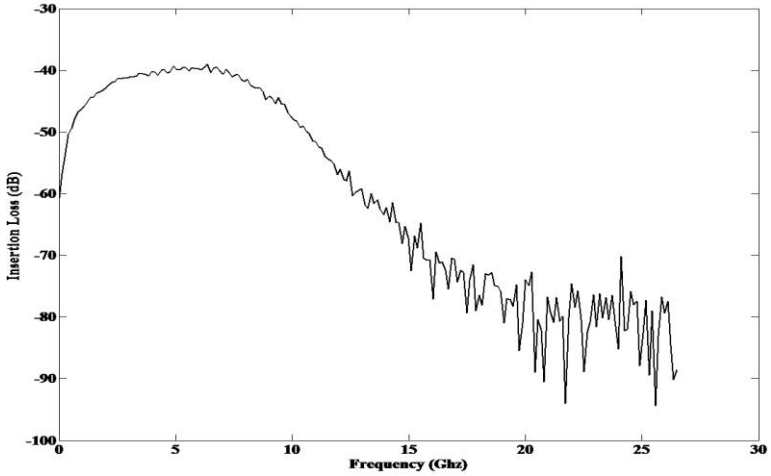


**Fig 8. S21 (dB) module NA with a wavelength λ=1548.38nm**

**5.2. Proving Tunability**

Next, we prove the tunability of the laser by slightly varying the wavelength in the first cut-off region. In Fig 9 it is seen how the low electrical frequency cutoff is changed when the wavelength is changed from 15471.19nm to 1547.23nm.

The previous results show that tunability of the low-frequency cutoff may be achieved. As seen, the higher cutoff is given by the maximum bandwidth of our Photodetector which is 10 GHz. From this

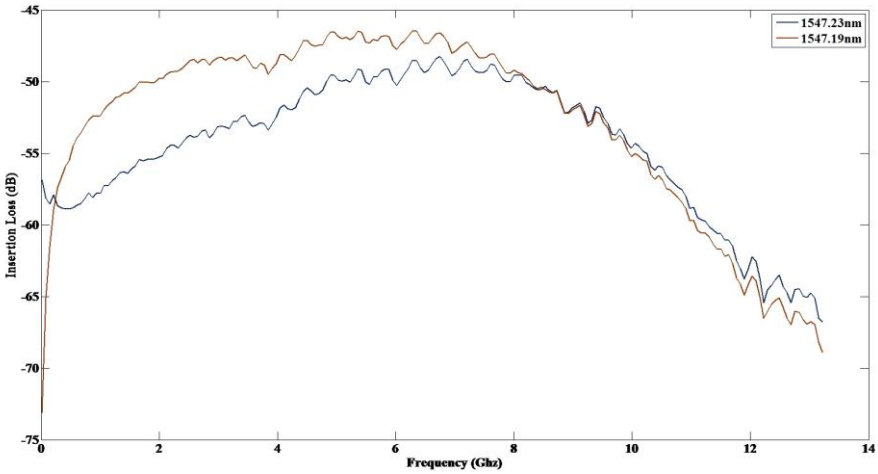


**Fig 9. Laser tunability performance in the wavelength λ=1547.19nm and λ= 1547.23nm**

result we anticipate that it will be very difficult to see that a second laser will allow us to control the high frequency cutoff. This cutoff on the other hand is a more critical cutoff as revealed by the simulations. Anyway we do the test and show results in the next section.

### 5.3. Combined test with both Lasers

After some time trying to show a passband response by using two lasers, the best result is that in Fig 10. This is not a very satisfactory result because by comparing with the rest of the measures, it is evident that our PD is the one imposing the high pass cutoff. The insertion loss value is very high as well. The conclusion is that in order to see the effect in our setup a higher BW PD is required, or else an optical filter with a steeper stop to passband transitions. In future experiments, the use of a 30GHz PD is envisioned. In this figure, the laser2 stays in the first cutoff with 19.83ºC equal to λ= 1547.10nm and laser 1 stays in the second cutoff λ=1548.38nm.

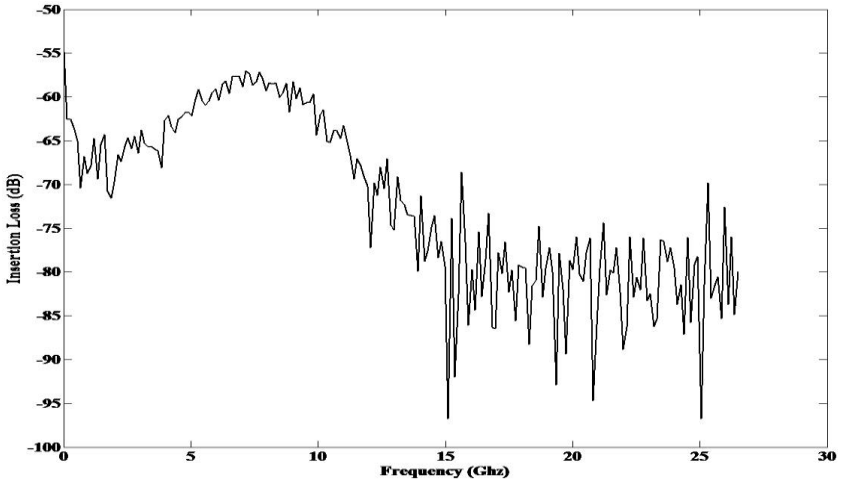


**Fig 10. S21(dB) module NA cut off of the second laser with 41.32mA power**

## 6. CONCLUSIONS

A novel scheme for the passband photonic filtering of signals in the microwave frequency range has been presented featuring both center frequency tunability and bandwidth adjustability. The microwave photonic filter proposed is simply reconfigured by control of the output wavelengths of

two laser sources and relies on a direct-synthesis approach based on microwave optical phase modulation and optical filtering and thus it possesses a single-passband response and is free from phase induced interference noise. It is also expected to lead to robust and compact setups which may exploit the maturity of fiber optic equipment developed for the telecom industry, holding promise for satellite applications.
Experimental results have demonstrated the high pass electrical filtering effect with low frequency cutoff tunability by changing the laser's wavelength, but due to the limited bandwidth of our PD a passband response by using two lasers could not be demonstrated. The use of a higher BW PD is envisioned in future works in order to show passband microwave photonic filters with independent control of the low and high cutoff frequencies by changes in the wavelength of one of the two lasers.

Simulations of the MPF have shown potential for broad center frequency tunability and bandwidth reconfigurability. The conducted research has revealed the key role played by both the optical filter spectral transfer characteristic and the input power levels, both in the optical as well as in the electrical domain, and work is presently under way in order to improve the stability of the setup and to identify optical filtering structures that could help to optimize the MPF characteristics. The simulations have shown that the MPFs high frequency cutoff is critical and that it probably depends on the dispersion characteristics of the optical filter used, which in the simulations was retrieved from the filter library of the simulation software. Further research will also have to look deeper into this issue trying different optical filter responses and analyzing the impact of the filter phase transfer characteristics into the MPF performance.

## 7. REFERENCES

[1] A. Bensoussan and M. Vanzi, "Optoelectronic devices productassurance guideline for space application," in Proceedings ofICSO 2010: International Conference on Space Optics (ESA,2010), pp. 8–13.
[2] M. Sotom, B. Benazet, A. Le Kernec, and M. Maignan,"Microwave photonic technologies for flexible satellitetelecom payloads," in Proceedings of the 35th EuropeanConference on Optical Communication, 2009 (IEEE, 2009),pp. 20–24.
[3] J. Capmany, J. Mora, I. Gasulla, J. Sancho, J. Lloret and S. Sales,"Microwave Photonic Signal Processing", J. of Lightw. Technol. vol.13, no. 4, Feb 2013.
[4] R. A. Minasian, "Photonic Signal Processing of Microwave Signals", IEEE Trans. Microw. Theory Tech., vol.54, no. 2, Feb 2006.
[5] J. Capmany, B. Ortega, D. Pastor, and S. Sales, "Discrete-time opticalprocessing of microwave signals," J. Lightw. Technol., vol. 23, no. 2,pp. 702–723, Feb. 2005
[6] X. Yi and R. A. Minasian, "Microwave Photonic Filter with single-bandpass response", Electron.Lett.,vol. 45, No. 7, March 2009. .
[7] D. Zhang, X. Feng and Y. Duang, " Tunable and Reconfigurable Bandpass Microwave Photonic Filters Utilizing Integrated Optical Processor on Silicon-on-Insulator Substrate", IEEE Photon. Technol. Lett., vol. 24, No. 17, Sept 2012.
[8] J. Palací, G.E. Villanueva, J. V. Galan, J. Marti and B. Vidal, IEEE Photon. Technol. Lett. Vol. 22, pp. 1276 (2010).
[9] W. Li, M. Li and J. Yao, " A Narrow-Passband and Frequency-Tunable Microwave Photonic Filter Based on Phase-Modulation to Intensity-Modulation Conversion Using a Phase-Shifted Fiber Bragg Grating", IEEE Trans. Microwave Th. And Tech., Vol 60, No. 5, May 2012.
[10] T. Chen ,X. Yi, L. Li and R. Minasian, "Single passband microwave photonic filter with wideband tunability and adjustable bandwidth", Optics Letters Vol. 37,No 22,pp 4699-4701, Nov 2012.
[11] VPI transmission maker, photonic modules reference manual. VirtualPhotonics Systems Inc. 2002.
[12] B. E. A. Saleh and M. C. Teich, "Fundamentals of Photonics", 2nd Edition, John Wiley & Sons, 2007.